Analysis of Warm Magnetic Measurements in a LHC Main Dipole Prototype

S. Gleis, J. Miles, O. Pagano, W. Scandale, E. Todesco.
CERN, LHC Division, CH-1211 Geneva 23, Switzerland

Abstract— **The data relative to the magnetic measurements at room temperature of the MBP2N1 prototype of the LHC dipole are presented. The measured field harmonics are compared to the results of the numerical model of the dipole cross section. The contribution from different effects are evaluated and compared to experimental data. Relevant quantities on the mechanical structure and on the expected field quality are worked out.**

I. Introduction

The 15-m long MBP2N1 LHC dipole prototype has a cross-section close to the one chosen for series production [1], i.e. 6-block coil design and collars without embedded magnetic insert, but featuring aluminum alloy collars (instead of austenitic steel ones) for reasons of component availability.

Magnetic measurements were performed at room temperature during the assembly and after the first powering tests. The results are used to study the field-shape performances of the dipole and to compare them with the expected values of the field harmonics computed with a magneto-static model [2]. References [3,4] inspired our analysis of the field-shape quality.

After a short description of the main features of the hybrid prototype in Section II, we present the results of the magnetic measurements in Section III. In Section IV we discuss them in detail. First, we distinguish between systematic and random effects. Then, we analyze the multipole changes induced by the thermal and powering cycle. Finally, we investigate correlation between multipoles measured at different stages of the dipole assembly. In Section V we present our conclusions.

II. Main Features of the Dipole

The 15-m long MBP2N1 prototype of the LHC main dipole features a cross-section close to the one chosen for series production, but for reasons of component availability, it is equipped with aluminum alloy collars instead of austentic steel ones. For the same reasons, the geometry of the collars, inserts and laminations is not the final one, thus making the contribution of the iron yoke to the dipole field-shape different from the design one.

The coil presents a 6-block geometry; it consists of an inner and an outer layer, each wound with a keystoned cable, as shown in Fig. 1. Wedge-shaped copper spacers are inserted between conductor blocks to correct the multipoles generated by the non-perfect cosine-θ geometry. The coil layers are assembled into poles, which in turn are assembled into dipoles. Magnetic coupling between the two apertures is a feature of the two-in-one design, leading to the presence of even harmonics (quadrupole, octupole, decapole,...) in the dipole field. The contribution of the iron yoke enhances the strength of the magnet and limits the field-shape imperfections.

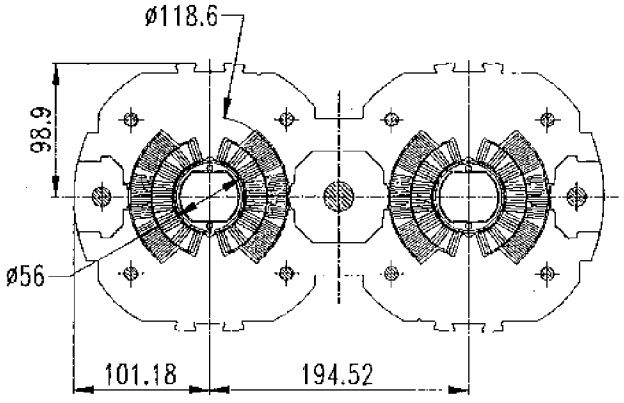

Fig. 1 Nominal design of the 6-blocks collared coil

III. Warm Magnetic Measurements

The magnetic measurements are made at room temperature using a probe containing 0.75 m long rotating coils. The field shape is described in terms of relative multipoles expressed at a reference radius R_{ref} = 17 mm, in units of 10^{-4}. At the selected excitation current of 20 A, the measurement sensitivity is expected to be of the order of 10^{-7} units. The field-shape is measured in both apertures, at 20 consecutive positions along the dipole length. However, the first and the last measurements are discarded to avoid fringe-field effects, since the first and the last positions include the dipole ends.

Measurements are performed on the collared coil, on the assembled cold mass and after the first cryo-powering test at high current. The results are summarized in terms of average and r.m.s. harmonics, computed over each aperture length. They are shown in Table I and II respectively.

During the measurement process, field harmonics induce a feed-down effect to lower harmonics if the mechanical axis of the measurement coil is not coincident with the magnetic axis of the harmonics themselves. In general the largest induced harmonics are one order below the driving harmonic and they are linearly proportional to the mechanical offset between the magnetic axis and that of the measuring coil. The design of the 6-block coil is such that:

Manuscript received on 27 September 1999

- The allowed harmonics b_{11}, b_{13}, b_{15}, and b_{17} are about a few 10^{-5} units at 17 mm reference radius.
- The non-allowed harmonics b_{10}, b_{12}, b_{14}, b_{16} and a_{10}, a_{12}, a_{14}, a_{16} are absent.
- Mechanical tolerances induce very small changes in the amplitude of harmonics greater than 10^{th} order.

TABLE I

MEASURED MULTIPOLES IN THE MBP2N1 PROTOTYPE: AVERAGE OF 18 MEASUREMENTS ALONG THE MAGNET AXIS. UNITS OF 10^{-4} AT R_{ref} = 17 mm.

	Collared		Assembled		After cryo	
	Ap. 1	Ap. 2	Ap. 1	Ap. 2	Ap. 1	Ap.2
a2	0.94	0.43	0.98	0.75	0.89	0.81
b2	-0.96	1.25	-5.48	5.73	-4.99	5.13
a3	-0.11	0.29	-0.38	-0.01	-0.46	0.00
b3	2.08	2.71	8.09	8.68	8.17	8.71
a4	0.06	0.05	0.05	0.10	0.07	0.11
b4	-0.07	0.20	-0.66	0.75	-0.67	0.77
a5	-0.06	-0.05	-0.07	-0.02	-0.08	-0.02
b5	-0.63	-0.60	-0.69	-0.64	-0.76	-0.71
a6	0.03	0.03	0.02	0.03	0.02	0.03
b6	0.00	-0.01	-0.02	0.03	-0.03	0.03
a7	0.03	0.03	0.02	0.00	0.02	0.01
b7	0.65	0.70	0.57	0.61	0.58	0.61
b9	0.25	0.26	0.26	0.26	0.21	0.20
b11	0.73	0.73	0.63	0.62	0.63	0.62

TABLE II

MEASURED MULTIPOLES IN THE MBP2N1 PROTOTYPE: STANDARD DEVIATIONS OF 18 MEASUREMENTS ALONG THE MAGNET AXIS. UNITS OF 10^{-4} AT R_{ref} = 17 mm.

	Collared		Assembled		After cryo	
	Ap. 1	Ap. 2	Ap. 1	Ap. 2	Ap. 1	Ap.2
a2	0.71	0.63	0.71	0.57	0.64	0.52
b2	0.36	0.43	0.39	0.44	0.40	0.46
a3	0.44	0.50	0.39	0.28	0.41	0.30
b3	0.39	0.39	0.34	0.32	0.31	0.33
a4	0.26	0.17	0.23	0.15	0.25	0.15
b4	0.14	0.13	0.12	0.11	0.12	0.11
a5	0.07	0.17	0.07	0.10	0.07	0.09
b5	0.13	0.12	0.13	0.11	0.13	0.11
a6	0.03	0.04	0.03	0.03	0.02	0.03
b6	0.08	0.06	0.07	0.04	0.07	0.05
a7	0.02	0.15	0.02	0.02	0.02	0.02
b7	0.06	0.03	0.05	0.03	0.05	0.03
b9	0.01	0.01	0.01	0.02	0.02	0.02
b11	0.00	0.00	0.01	0.00	0.01	0.00

It is natural to determine the local magnetic centre at different longitudinal positions in each aperture by assuming that the non-allowed harmonics are only due to first order feed-down of odd normal harmonics according to:

$$b_{2n} = 2n b_{2n+1} \frac{x_0(n)}{R_{ref}} \qquad a_{2n} = 2n b_{2n+1} \frac{y_0(n)}{R_{ref}}$$

where n = 5, 6, 7, 8. It follows that the magnetic centre (x_o, y_o) is given by :

$$x_0(n) = R_{ref} \frac{b_{2n}}{2n b_{2n+1}} \qquad y_0(n) = R_{ref} \frac{a_{2n}}{2n b_{2n+1}}$$

We identified the offset between the axis of the rotating coil and the magnetic axis by applying these formulae to the feed down of b_{17} in each aperture and in each axial position and we subtracted its effect in the results of Tables I and II.

IV. ANALYSIS OF THE DATA

A. Systematic Effects

The data of Table I have been compared with the multipoles expected in the nominal collared coil, see Table III, and in the nominal assembled cold mass, see Table IV.

The simulations neglect the following contributions to the field-shape errors:

- Geometrical tolerances of the collars and coils.
- Deformations induced by mechanical stress during manufacturing.

TABLE III

MULTIPOLES IN THE COLLARED DIPOLE: NUMERICAL SIMULATIONS VERSUS EXPERIMENTAL DATA FOR BOTH APERTURES. UNITS OF 10^{-4} AT R_{ref} = 17 *mm*.

	Simulations	Difference to measurements	
		Ap. 1	Ap. 2
b2	0.00	-0.96	1.25
b3	4.16	2.08	1.45
b5	-0.98	-0.35	-0.38
b7	0.80	0.15	0.10
b9	0.15	-0.10	-0.11
b11	0.72	-0.01	-0.01

The first effect is the same for the collared coil and for the assembled cold mass. The second one is in principle different since the yoke transmits an additional stress to the coils. In our case this fact can be rather relevant since the collar is in aluminum. Indeed, the values of columns 3 and 4 in Table III are rather different from those in Table IV and it is not yet clear if this can be interpreted only in terms of the increased deformation induced by the yoking process. This discrepancy is at present the limit of our model for field-shape error estimates.

The simulated multipoles agree with the averages within ± 3·standard deviations (see Tables II and III) of the measured data, with the only exceptions of b_4 and b_9. Corrective actions may be needed if this offset will persist and if it will appear to be detrimental for the circulating beam.

TABLE IV

MULTIPOLES IN THE ASSEMBLED DIPOLE: NUMERICAL SIMULATIONS VERSUS EXPERIMENTAL DATA FOR BOTH APERTURES. UNITS OF 10^{-4} AT R_{ref} = 17 *mm*.

	Simulations	Difference to measurements	
		Ap. 1	Ap. 2
b2	4.25	-1.23	-1.48
b3	7.32	-0.77	-1.36
b4	0.00	-0.66	-0.75
b5	-1.05	-0.36	-0.41
b7	0.63	0.06	0.02
b9	0.10	-0.16	-0.16
b11	0.61	-0.02	-0.01

B. Random Effects

Random multipoles can be interpreted in terms of random displacement of the blocks. In Ref [5] it is shown that this interpretation gives rise to a very simple scaling law for the induced multipoles. The standard deviation σ_n of the multipole distribution of order n scales linearly with the amplitude of the random displacement d according to the following three-parameter expression:

$$\log_{10} \sigma_n = a + b\, n + c\, n^2,$$

or equivalently

$$\sigma_n = A \cdot B^n \cdot C^{n^2},$$

with a, b and c (or A, B and C) independent of d. In addition, normal and skew components of the same order n have about the same standard deviation σ_n.

The standard deviations of Table II can thus be compared to the predictions of the multipole scaling law, assuming independent block displacements normally distributed, with zero mean and standard deviation d along the dipole axis. In Fig. 2 the experimental data are compared to simulations obtained by varying d from 6 to 100 μm. The observed multipoles are compatible with a value of d in the range of 6 to 25 μm, such as in the previous 5-block coil prototypes [5]. This implies that the geometrically induced random multipoles are the same in the 5-block and in the 6-block coil design.

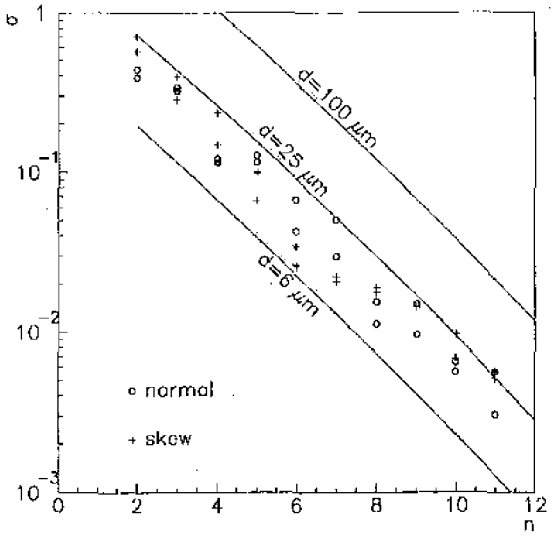

Fig. 2. Standard deviation of random multipoles versus harmonic order n: Experimental data (dots) and numerical simulations for different amplitudes of random displacements d (solid curves).

C. Effect of Cycle to Cryogenic Temperature

The shift of the average multipole harmonics measured at room temperature before the first cryogenic and powering test are shown in Table V. The effect is very small compared to that observed in the 5-block prototypes [5].

If we try to interpret it in terms of systematic movements of the blocks we find displacements of the order of a few tens of μm, i.e. of the same order as the random displacements discussed in Subsection *B*.

In comparison, coherent movements of about 50 μm were deduced from the average multipole shifts observed in the 5-block coil prototypes [5]. This result confirms that the present 6-block coil design is mechanically more stable than the previous 5-block coil design.

TABLE V

DIFFERENCES IN MULTIPOLES BETWEEN BEFORE AND AFTER THE FIRST THERMAL CYCLE, FOR BOTH APERTURES. UNITS OF 10^{-4} AT R_{REF} = 17 *mm*.

	Ap. 1	Ap. 2
a2	-0.09	0.06
b2	-0.49	-0.60
a3	-0.08	0.01
b3	0.07	0.03
a4	0.02	0.01
b4	-0.01	0.02
a5	-0.01	0.00
b5	-0.07	-0.07
a6	0.00	0.00
b6	-0.01	0.00
a7	0.00	0.01
b7	0.01	0.00
b9	-0.05	-0.06
b11	-0.00	0.00

D. Correlation between Multipoles

In Table VI we quote correlation between multipoles measured along the dipole axis, in the two apertures, for the collared coil and the cold mass. A linear law, as shown in Figs. 3, 4 and 5 for the harmonics b3, b5 and a2, respectively, very well interpolates experimental results. The coefficients p and q in Table VI are the slope and the ordinate at the origin of the interpolating line and r is the correlation coefficient for the experimental data.

TABLE VI

CORRELATION BETWEEN RELEVANT MULTIPOLES, COLLARED COILS AND ASSEMBLIES; INTERPOLATION CONSTANTS q AND p, AND CORRELATION COEFFICIENT r.

	q	p	r
a2	0.10	0.99	0.98
b2	-4.52	0.98	0.93
a3	-0.20	0.86	0.95
b3	6.30	0.82	0.97
a4	0.04	0.85	0.95
b4	-0.58	0.84	0.97
b5	-0.08	0.96	0.99
b7	-0.03	0.86	0.99

The slope p is always close to one: this implies that the main effect of the yoke assembly is a shift of the harmonics that is particularly significant for b_2, b_3 and b_4.

We observe that the correlation is always excellent and that the harmonics have the same behavior in both apertures. This gives us confidence that measurements made in the collared coils give a reliable early indication of the field-shape quality to be expected in the final cold mass. Of course, this indication can be exploited to propose an economic and efficient quality control process during series production. The identification of corrective actions is still limited by the phenomenon discussed in Subsection *A*. Further studies in the final dipole design with stainless steel collars may clarify this point.

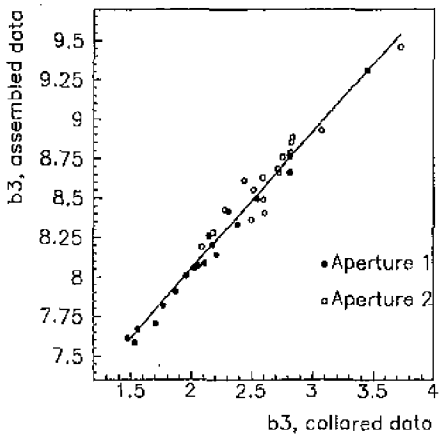

Fig. 3. Correlation of b_3, collared coil versus assembled cold mass data (18 measurements along the dipole axis for both apertures). Units of 10^{-4} at $R_{ref} = 17$ mm

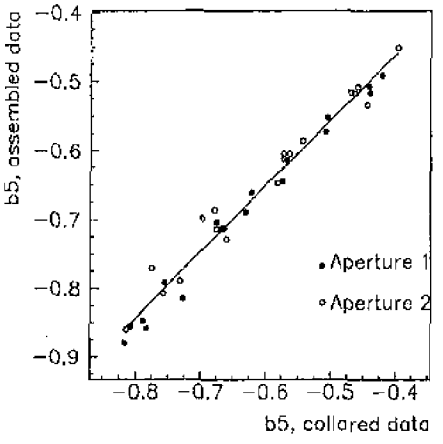

Fig. 4: Correlation of b_5, collared coil versus assembled cold mass data (18 measurements along the dipole axis for both apertures). Units of 10^{-4} at $R_{ref} = 17$ mm

V. Conclusion

We discussed the magnetic measurements of the MBP2N1 dipole prototype. Although this magnet still differs from the final LHC dipole design, we could obtain numerous information that is expected to hold in general.

The order of magnitude of the systematic field-shape errors induced by geometrical imperfections is rather well predicted. The random variations of the multipoles along the dipole axis are quite limited and are induced by small geometrical misplacements of the conductors, characterized by a standard deviation in the range of 6 to 25 μm. In this respect the 5- and 6-block coil designs are identical. On the other hand, the coil deformation induced by the first cryogenic test of the dipole at high current is almost negligible. This confirms that the 6-block design is very stable and almost immune to systematic block movements, contrary to what was previously observed in the 5-block coil [5].

The strong correlation observed in the field harmonics of the collared coil and of the fully assembled cold mass opens the way to an economic and efficient strategy of field-shape quality control during series production.

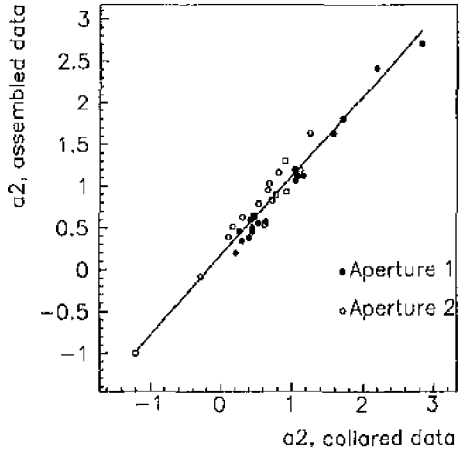

Fig. 5: Correlation of $a2$, collared coil versus assembled cold mass data (18 measurements along the dipole axis for both apertures). Units of 10^{-4} at $R_{ref} = 17$ mm.

References

[1] K. Artoos et al., Design, manufacturing status, first results of the LHC main dipole final prototypes and steps towards series manufacture, these Proc.

[2] S. Russenschuck, ed., CERN 99-01, 1999.

[3] R. Gupta et al., Field Quality Analysis as a Tool to Monitor Magnet Production, MT-15, Beijing, China, October 20-24, 1997.

[4] P. Schmüser, DESY HERA-P, 92-1, 1992.

[5] O. Pagano, W. Scandale, E. Todesco, LHC Project Note 180.